Defence Science Journal, Vol. 69, No. 4, July 2019, pp. 353-360, DOI : 10.14429/dsj.69.13607

Behavioural Fault-tolerant-control of an Omni-directional Mobile Robot with Four-mecanum Wheels

Swati Mishra[#], Mukesh Sharma[@], and M. Santhakumar[$,*]

[#]*Indian Institute of Technology, Indore - 453 552, India*
[@]*Indian Institute of Technology, Jodhpur - 342 037, India*
[$]*Indian Institute of Technology, Palakkad - 678 557, India*
[*]*E-mail: santhakumar@iitpkd.ac.in*

ABSTRACT

This paper analyses the four-mecanum wheeled drive mobile robot wheels configurations that will give near desired performance with one fault and two faults for both set-point control and trajectory-tracking (circular profile) using kinematic motion control scheme within the tolerance limit. For one fault the system remains in its full actuation capabilities and gives the desired performance with the same control scheme. In case of two-fault wheels all combinations of faulty wheels have been considered using the same control scheme. Some configurations give desired performance within the tolerance limit defined while some does not even use pseudo inverse since using the system becomes under-actuated and their wheel alignment and configurations greatly influenced the performance.

Keywords: Omni-directional; Mecanum wheel; Differential-drive; Fault-tolerant-control; Line-of-sight; Kinematic control

1. INTRODUCTION

At present, automated mobile platform has become a major part of human life since they are extensively used in industrial, domestic, agricultural, educational, research, defence, etc. Some of the most common examples are wheel chair, service robot, rescue robots, robots in warehouse, etc. that aims at facilitating human physical disabilities, robots in warehouse for inspection, monitoring crowd, product handling in factories, patrolling the boarder, etc.

The wheels currently being used are: traditional wheel, Omni-directional wheel and mecanum wheel, each having their own merits and demerits.

A huge bulk of research effort has been put on developing robust omni-directional mobile robot using mecanum wheels due to its enhanced mobility. This quest for exploiting merits of mecanum wheel is since 1972, when the mecanum wheels were introduced for the first time. The effort of the researchers led in designing of mobile robot with mecanum wheels[1] kinematic modelling along with improvement of mecanum wheels[2-8], also a step ahead has been taken in developing control[9] and dynamic model[10] techniques for estimating unknown model parameters[11] for this type of robots. In critical conditions such as rescuing operations etc. where the chance of the failure of the actuators increases drastically. Therefore, it is needed to increase their robustness against possible actuator failure. In some cases, actuator failure causes unnecessary accelerations and forces which are highly dangerous for the mobile robot as well as people nearby. So, it is of prime importance for autonomous robot to first identify the fault and take suitable remedial to prevent any catastrophe. Some effort has been made to identify faults[12-13] and to minimise their effect in the performance of mobile robot. Generally, minor faults are compensated in closed loop control by their feedback but so is not the case in open loop.

The four-mecanum wheel drive mobile robot, under the failure of one actuator the system remains in full actuation capability and can operate to full potential. This make the system good for testing fault tolerant control (FTC) methods. There exists some FTC techniques[12-16] and work which incorporates FTC for performance optimisation[17-18]. The existing techniques mainly deals with passive and active approach where in one case inherent fault is assumed in the system and the control law is used accordingly while the other tries to minimise the deviation from the desired performance using some pre-built control law or onboard computation. Some FTC techniques incorporates line-of-sight[19-21] (LOS) in which system becomes under-actuated due to failure of a greater number of actuators than the state variables.

This paper studies the behaviour of four-mecanum wheel drive mobile robot without fault, with one-fault, with two-fault and then addresses the FTC technique using kinematic control scheme for both set-point control and trajectory tracking control (circular profile). In our paper we are trying to find the best configurations of the four-mecanum wheel drive mobile robot with the different cases of fault. For two fault cases, the system has been treated as differential drive model[22-23], while with one-fault the issues have been dealt using weighted pseudo-inverse. The system can be studied further for three faults in which it

Received : 11 September 2018, Revised : 03 April 2019
Accepted : 30 April 2019, Online published : 15 July 2019

shall be treated as unicycle model[24] which would be complex and has been left for further research.

2. SYSTEM DESCRIPTION

The mecanum wheels consist of freely rotating small rollers, symmetrically distributed on their hub, having three degrees of freedom. Therefore, as the wheels rotate about the drive shaft and rollers about their axis, the wheels can move in one direction and allow free motion in another. Figure 1 shows JR-2 vehicle-manipulator in lab environment. Figure 2 shows the major dimensions of the JR-2 vehicle-manipulator.

Figure 1. Photographic image of the JR-2 vehicle-manipulator in lab environment.

Figure 2 presents the possible configurations of the omni-directional mobile robot with four mecanum wheels. The mobile platform considered has four mecanum wheels evenly distributed around the centre of mass, moving in a two-dimensional space i.e. translation in x, y axis and rotation about z axis of the inertial frame {I}. $\eta \in \Re^{3\times1}$ is the vector of mobile base positions and orientations namely $\eta = [x \quad y \quad \varphi]^{\mathrm{T}}$. $\hat{\imath} \in \Re^{3\times1}$ is the vector of velocity inputs in body-fixed coordinate frame of the mobile base which is given as $\hat{\imath} = [u \quad v \quad r]^{\mathrm{T}}$. Other three more such platforms have been taken for investigation with different wheels configuration (See Fig. S1, Table S1, Fig. S2 provided in supplementary material).

One fault implies that one of the actuator is not being actuated or functional, while two fault means two actuators are not actuated or functional. For two fault cases, there are six possible cases where the faults can occur {(1,2), (1,3), (1,4), (2,3), (2,4), (3,4)} where 1,2,3,4 are the actuator numbers and each ordered pair represent set of actuators that fails.

3. KINEMATIC MODELLING

3.1 Forward Kinematics

The mobile base considered has wheels numbered 1, …, 4. (See Fig. S2(a)). Let's assume the angular velocities of the wheels as q_i, i = 1, …,4, while the velocities of the centre of mass u, v and r expressed in frame {CG} attached to it. Let the tangential velocities of the free roller touching the floor as ν_{ir}, i = 1, …,4. Then from [3], we have the resultant wheel velocity as:

$$\begin{aligned}
\nu_{1x} &= \nu_{1w} + \nu_{1r}\sin\phi, \quad \nu_{1y} = -\nu_{1r}\cos\phi \\
\nu_{2x} &= \nu_{2w} + \nu_{2r}\sin\phi, \quad \nu_{2y} = \nu_{2r}\cos\phi \\
\nu_{3x} &= \nu_{3w} + \nu_{3r}\sin\phi, \quad \nu_{3y} = -\nu_{3r}\cos\phi \\
\nu_{4x} &= \nu_{4w} + \nu_{4r}\sin\phi, \quad \nu_{4y} = \nu_{4r}\cos\phi
\end{aligned} \tag{1}$$

where ϕ is the angle between the axis of the wheel and the axis of the roller, for a typical offset angle ϕ =45°. Also, the wheels are rigidly attached to the body so their velocities can be related to the velocities of the mobile platform as:

$$\begin{aligned}
\nu_{1x} &= u - dr, \quad \nu_{1y} = v + Lr \\
\nu_{2x} &= u - dr, \quad \nu_{2y} = v - Lr \\
\nu_{3x} &= u + dr, \quad \nu_{3y} = v - Lr \\
\nu_{4x} &= u + dr, \quad \nu_{4y} = v + Lr
\end{aligned} \tag{2}$$

where L and d represents the longitudinal and lateral distance of wheel from the centre of mass respectively. Solving (2) with respect to the body velocities u, v and r substituting $\nu_{iw} = a\dot{q}i$, i = 1, …,4, and ϕ =45°, get the forward kinematics of the platform as:

$$\xi = Bk \tag{3}$$

where, B is a rectangular Jacobian matrix and $k = \left[\dot{q}_1, \dot{q}_2, \dot{q}_3, \dot{q}_4\right]^T$ can be defined as wheel angular velocities. Now, the body velocities can be expressed in inertial frame by:

$$\dot{\eta} = J(\eta)\xi \tag{4}$$

where x, y and φ represents the position and orientation of the mobile platform with respect to the inertial frame and $J \in \Re^{3\times1}$ which is a Jacobian matrix expressed as:

$$J = \begin{bmatrix} \cos\varphi & -\sin\varphi & 0 \\ \sin\varphi & \cos\varphi & 0 \\ 0 & 0 & 1 \end{bmatrix} \tag{5}$$

3.2 *Inverse Kinematics*

From (3), (4) and (5) we get:

$$\dot{\eta} = JBk \tag{6}$$

which is the equation for the forward kinematics then the equation for the inverse kinematics is as:

$$k = B^{+}J^{T}(\dot{\eta}) \tag{7}$$

where

$$B^{+} = B^{T}(BB^{T})^{-1} \tag{8}$$

using Moore-Penrose Pseudo Inverse since the matrix $B \in \Re^{3\times4}$.

In case of one-fault matrix $B \in \Re^{3\times3}$ and hence simple pseudo inverse[25] will be sufficient provided it is not singular matrix. For the two-fault case for the matrix B becomes

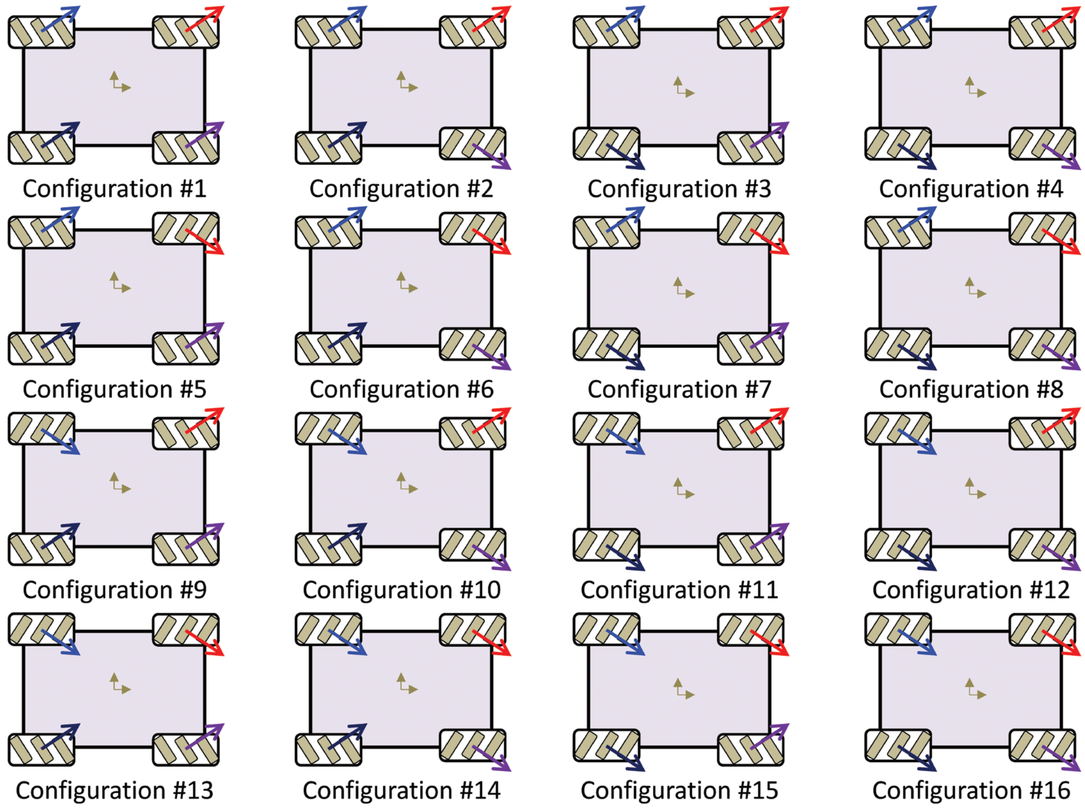

Figure 2. Possible configurations of the omni-directional mobile robot with 4-mecanum wheels.

$B \in \Re^{3\times2}$ and hence simple inverse is not possible. So, using Moore-Penrose Pseudo Inverse:

$$B^{+} = (B^{T}B)^{-1}B^{T} \tag{9}$$

Performance matrix H can be introduced as a diagonal matrix written as:

$$H = \begin{bmatrix} \lambda1 & 0 & 0 & 0 \\ 0 & \lambda2 & 0 & 0 \\ 0 & 0 & \lambda3 & 0 \\ 0 & 0 & 0 & \lambda4 \end{bmatrix} \tag{10}$$

where $0 <= \lambda_i <= 1,\ i = 1, ..., 4$. Here λ is the performance measure of actuator where $\lambda_i = 1$ means i^{th} actuator is perfectly working while $\lambda_i = 0$ means i^{th} actuator is non-functional while actuator is partially malfunctioned than λ can be assigned any value between 0 and 1 accordingly. Then the matrix B in (9) shall be replaced by (BH) where $(BH)^{+}$ will be weighted pseudo inverse[26] which is given below:

$$(BH)^{+} = (BH)^{\mathrm{T}}\left((BH)(BH)^{\mathrm{T}}\right)^{-1} \tag{11}$$

Likewise, health matrix for the actuators in case of one-fault or two-fault can also introduce just as their dimension reduces to $H \in \Re^{3\times3}$ and $H \in \Re^{2\times2}$ respectively.

4. KINEMATIC CONTROL DESIGN

In this research computed velocity control is implemented to achieve the ultimate aim to follow the desired operational space pose vector trajectory of the vehicle manipulator with uncertainties and time varying external disturbances. In order to perform motion control, kinematic control scheme used in this article is as:

$$\xi = J^{-1}[\dot{\eta}_d + K_p(\eta_d - \eta)] \tag{12}$$

$\dot{\eta}_d$ is the vector of desired inertial frame (earth-fixed) configuration-space velocities which is obtained from the desired operational-space velocities. $\tilde{\eta} = \eta_d - \eta$ is the vector of configuration-space pose errors. η_d is the desired configuration-space pose vector. η is the actual configuration-space pose vector. K_p is the controller gain matrix and chosen as a symmetric positive definite matrix, that is, $K_p = K_p^{\mathrm{T}} > 0$. $J^{-1} \in \Re^{3\times1}$ is the vector of inverse of Jacobian matrix. To correlate the generalised input velocity vector with the individual actuator inputs (rotational speeds) of the system, the input (control) vector can be rewritten as:

$$\xi = Bk \tag{13}$$

here, B is the actuator configuration matrix and k (kappa) is the vector of actuator velocity inputs. Figure 3 presents the flowchart representation of the fault tolerant control scheme. Figure S3 shows the methodology and Fig. S4 explains the fault tolerant control scheme with the help of algorithmic representation provided in the supplementary material.

5. TESTING AND OUTCOMES

The kinematic control on the mobile platform has been tested using MATLAB simulation environment in real-time without random noise. Line-of-sight method has been used for two-fault case.

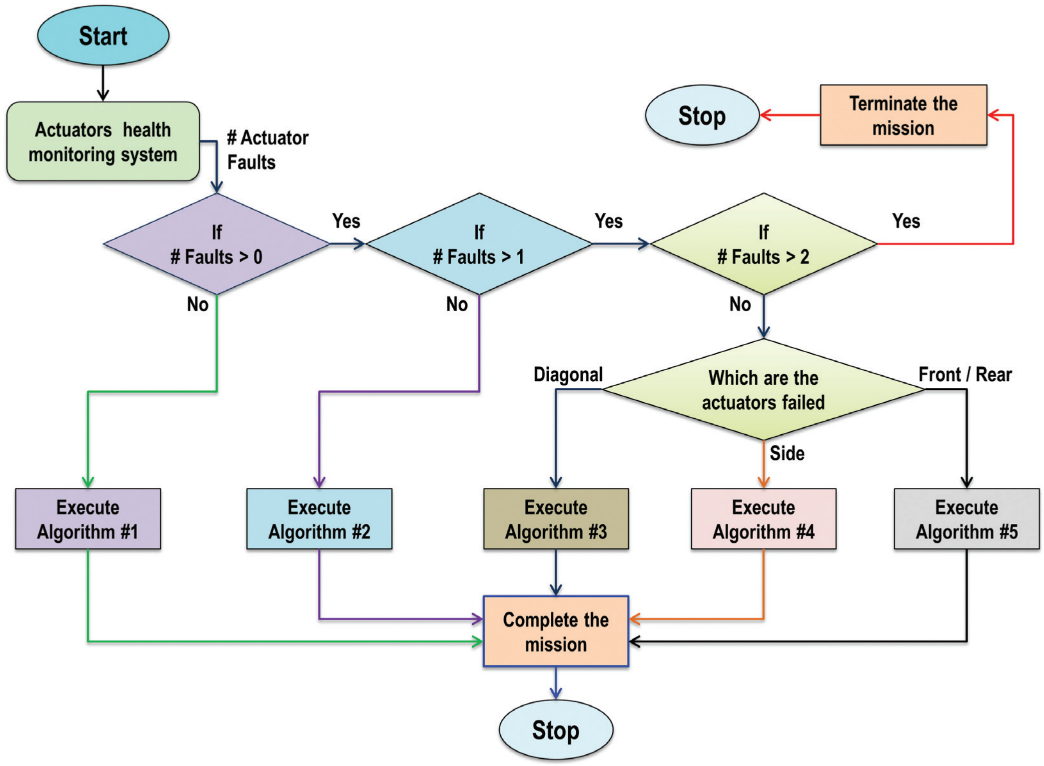

Figure 3. Flowchart representation of the proposed fault tolerant control scheme.

5.1 No-Fault Case

The objective is to make mobile robot to follow a trajectory (circular profile), since the mobile robot is over-actuated this is simply done by using Moore-Penrose Pseudo-Inverse to get to the angular velocities of the actuators from equation mentioned below:

$$k = B^{+} J^{\mathrm{T}} (\dot{\eta}) \tag{14}$$

where $B^{+} = B^{T}\left(BB^{T}\right)^{-1}$. The kinematic control was tested tuning the proportionality gain. Initial error in the graph is because the mobile robot is not positioned and oriented on the desired trajectory.

5.2 One-Fault Cases

In case one of the actuators fails and failure has been detected the following proposed method can be used. Here, the desired wheel velocity can be calculated by using:

$$k = B^{+} J^{\mathrm{T}} (\dot{\eta}) \tag{15}$$

where $B^{+} = B^{-1}$ since B is a square matrix of $B \in \Re^{3\times 3}$. Kinematic control scheme with designed FTC method is used to make mobile robot follow circular trajectory. There are four possible cases since either of the actuators can fail and the mobile robot would behave differently. For one-fault case both pseudo inverse and weighted pseudo inverse has been used. The proportionality gain for both the cases is 2 and it has been assumed that the actuator-1 fails after 20 seconds for the wheel configuration-4. Here x_e and y_e represents the error in x, y positions, Ψ_e represents the error in orientation and P_e represents the total error in the position of the robot. The velocity of the Mecanum wheel platform considered is of sinusoidal nature having amplitude of 0.2 m/s and the distance covered is 13 meters.

The Table 1 shows that error in position is about 0.8 per cent when weighted pseudo inverse is used which is easily tolerable, however error is bit more in case of pseudo inverse. Figure 4 shows that effect of an actuator failure on rest of three functional actuators.

For circular trajectory (one fault case)

Table 2 presents the corresponding mean errors of the vehicle positions for circular trajectory in one fault case. Figure S5 shows the desired and actual path followed by the robot. Figure S6 shows the steady state error for both the x and y positions for the one fault case.

Table 1. Corresponding root mean square (RMS) errors of the vehicle positions

Parameters	RMS position error (m)							
	Actuator-1 failure		Actuator-2 failure		Actuator-3 failure		Actuator-4 failure	
	x_e	y_e	x_e	y_e	x_e	y_e	x_e	y_e
With fault with pseudo inverse	0.027	0.034	0.111	0.013	0.011	0.135	0.030	0.031
With fault with weighted pseudo inverse	0.006	0.008	0.006	0.008	0.006	0.008	0.006	0.008

Table 2. Corresponding mean errors of the vehicle positions

Parameters	Mean position error (m)							
	Actuator-1 failure		Actuator-2 failure		Actuator-3 failure		Actuator-4 failure	
	x_e	y_e	x_e	y_e	x_e	y_e	x_e	y_e
With fault with pseudo inverse	-0.013	0.004	-0.005	0.003	0.003	-0.001	0.009	-0.007
With fault with weighted pseudo inverse	-0.001	0.001	0.001	0.001	0.001	0.001	-0.001	0.001

Considering one of the cases

With one-faulty wheel, using pseudo inverse, the mobile robot does not attain the steady state, however using the weighted pseudo inverse technique, the steady state error reduces to about 0.0005 meter for the both the x and the y positions.

5.3 Two-Fault Cases

In case of two-faults, the system becomes under-actuated and it is not feasible to obtain both position and orientation of the platform in two-dimensional space simultaneously and therefore line-of-sight method has been used along with kinematic control scheme. For the rectangular matrix, Moore-Penrose Pseudo inverse has been use where actuator matrix will have the elements corresponding to the actuators which are functional.

5.3.1 Set-point Control

Initially the analysis was done for set-point control scheme to check whether the platform reaches the desired set-point. The initial position of the mobile robot was (0,0) and the desired point was for all the cases of different wheel configurations and the desired wheel velocity was calculated using:

$$k = B^{+} J^{\mathrm{T}} (\dot{\eta}) \tag{16}$$

where, $B \in \Re^{3\times 2}$ and $B^{+} = \left(B^{T} B\right)^{-1} B^{T}$. The proportionality gain is 2 for all the cases. The results have been shown in Fig. 5 for wheel configuration 6 and detailed results for other configurations has been provided in Fig. S7. Corresponding Root Mean Square error has been tabulated with four different configurations of the mobile robot shown in Table 3.

5.3.2 Trajectory-tracking Control

After testing for set-point control scheme, this was further extended to trajectory tracking where circular profile is considered and line-of-sight method has been used with the kinematic control scheme. The resulting wheel velocity was obtained from equation which can be expressed as:

$$k = B^{+} J^{\mathrm{T}} (\dot{\eta}) \tag{17}$$

where $B \in \Re^{3\times 2}$ and $B^{+} = \left(B^{T} B\right)^{-1} B^{T}$. The proportionality gain is tuned as earlier cases and Moore-Penrose Pseudo inverse has been used. The results analysed for wheel configuration 4 is given in Fig. 6 and results for remaining wheel configuration is shown in Fig. S8 . Similarly, the corresponding Root Mean Square Error values have been calculated with four different configurations of the mobile robot as presented in Table 4.

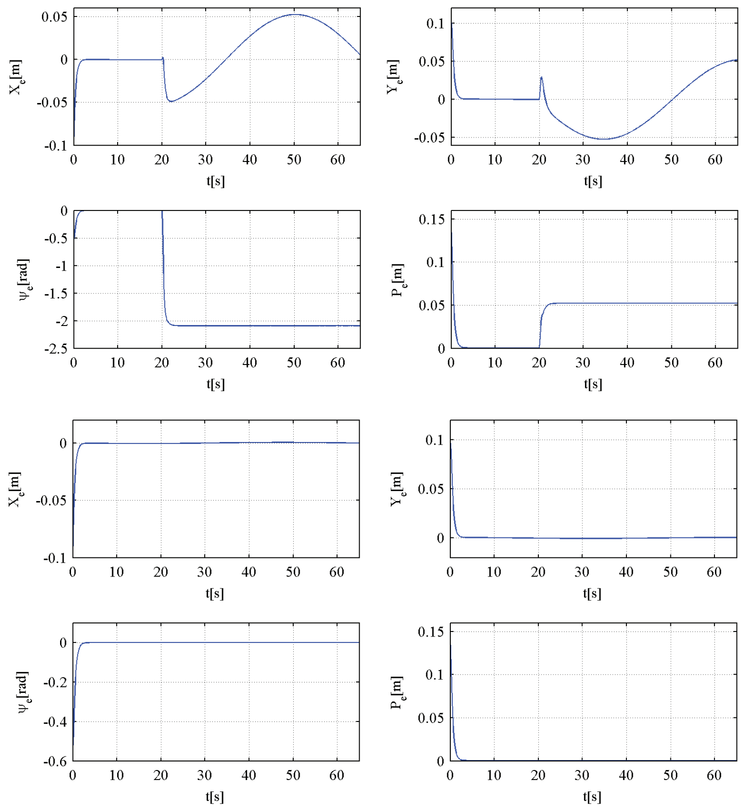

Figure 4. Time trajectory of the tracking errors of the mobile robot with single actuator faults (a) Error incurred with normal pseudo inverse in one fault situation and (b) Error incurred with weighted pseudo inverse in one fault situation.

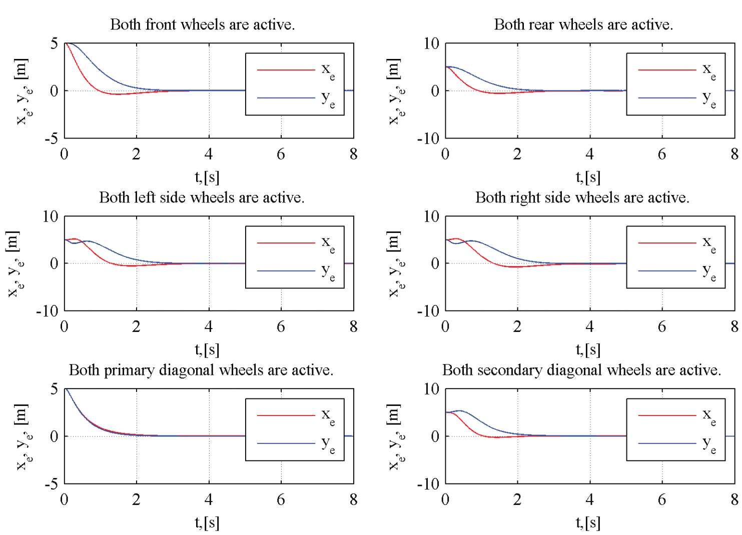

Figure 5. Tracking position errors of the robot during set-point control task with two actuator faults.

Table 3. RMS values of the error for different cases of four-wheel configuration

(a) Wheel-configuration 1

Cases	RMS error(m)	
	X_{e_RMS}	Y_{e_RMS}
Both front wheels are active	0.980	1.192
Both rear wheels are active	0.967	1.521
Both left side wheels are active	1.187	1.578
Both right side wheels are active	1.227	1.362
Both primary diagonal wheels are active	1.357	2.065
Both secondary diagonal wheels are active	1.071	1.004

(b) Wheel-configuration 2

Cases	RMS error(m)	
	X_{e_RMS}	Y_{e_RMS}
Both front wheels are active	0.951	1.462
Both rear wheels are active	1.183	1.308
Both left side wheels are active	1.227	1.362
Both right side wheels are active	1.187	1.578
Both primary diagonal wheels are active	1.234	1.871
Both secondary diagonal wheels are active	1.019	1.050

(c) Wheel-configuration 3

Cases	RMS error(m)	
	X_{e_RMS}	Y_{e_RMS}
Both front wheels are active	0.980	1.192
Both rear wheels are active	1.012	1.731
Both left side wheels are active	1.192	0.979
Both right side wheels are active	1.183	1.308
Both primary diagonal wheels are active	1.247	1.921
Both secondary diagonal wheels are active	1.042	1.026

(d) Wheel-configuration 4

Cases	RMS error(m)	
	X_{e_RMS}	Y_{e_RMS}
Both front wheels are active	0.951	1.462
Both rear wheels are active	0.967	1.521
Both left side wheels are active	1.462	1.779
Both right side wheels are active	1.540	1.882
Both primary diagonal wheels are active	1.042	1.026
Both secondary diagonal wheels are active	1.247	1.921

Table 4. RMS Errors for different cases during trajectory tracking control

(a) Wheel-configuration 1

Cases	RMS error (m)	
	X_{e_RMS}	Y_{e_RMS}
Both front wheels are active	0.280	0.271
Both rear wheels are active	0.067	0.075
Both left side wheels are active	0.068	0.071
Both right side wheels are active	0.034	0.034
Both primary diagonal wheels are active	0.079	0.080
Both secondary diagonal wheels are active	0.027	0.028

(b) Wheel-configuration 2

Cases	RMS error (m)	
	X_{e_RMS}	Y_{e_RMS}
Both front wheels are active	0.015	0.017
Both rear wheels are active	0.252	0.257
Both left side wheels are active	0.034	0.034
Both right side wheels are active	0.068	0.071
Both primary diagonal wheels are active	0.062	0.061
Both secondary diagonal wheels are active	0.063	0.065

(c) Wheel-configuration 3

Cases	RMS error(m)	
	X_{e_RMS}	Y_{e_RMS}
Both front wheels are active	0.280	0.271
Both rear wheels are active	0.252	0.257
Both left side wheels are active	0.251	0.256
Both right side wheels are active	0.314	0.313
Both primary diagonal wheels are active	0.233	0.251
Both secondary diagonal wheels are active	0.205	0.223

(d) Wheel-configuration 4

Cases	RMS error(m)	
	X_{e_RMS}	Y_{e_RMS}
Both front wheels are active	0.015	0.017
Both rear wheels are active	0.067	0.075
Both left side wheels are active	0.040	0.040
Both right side wheels are active	0.073	0.074
Both primary diagonal wheels are active	0.166	0.185
Both secondary diagonal wheels are active	0.250	0.267

Since the system is under-actuated, concern is about position error not orientation as both cannot be achieved simultaneously. The tolerance limit varies between 5 per cent to about 30 per cent. Analysis for those roller angles has been left for further research.

6. DELIBERATIONS

Kinematic control scheme with proposed FTC is found quite effective for the four-mecanum wheeled drive mobile robots for both set-point control and trajectory-tracking control. For inverse kinematics pseudo inverse is found less effective than weighted pseudo inverse, error is relatively smaller using weighted pseudo inverse than pseudo inverse as depicted in Fig. 4(a, b). Likewise, the modification of four-mecanum wheeled mobile platform to differential drive system for two fault cases is effective compared to modification of the platform to unicycle model. It has been considered that the fault has already been detected and hence this topic has not been brought into picture.

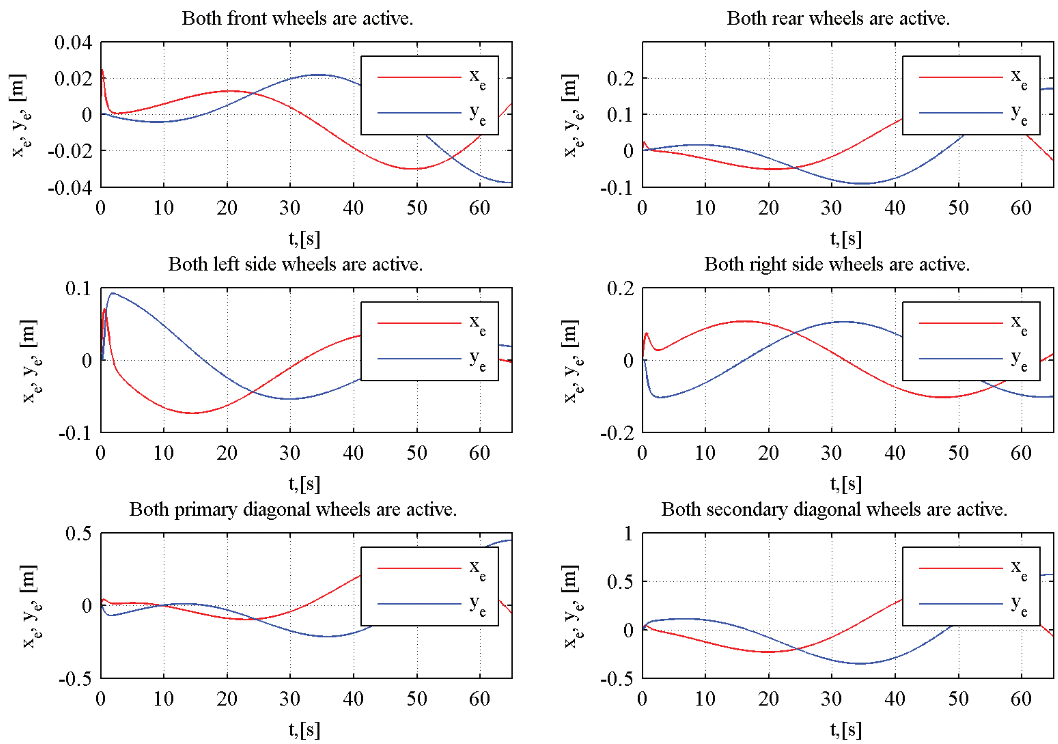

Figure 6. Tracking errors of the robot during circular profile tracking task with two actuator faults.

7. CONCLUSIONS

In this paper an analysis on the behavior of four-mecanum wheeled drive mobile robot for one-fault and two-fault conditions with FTC has been presented. The analysis presented is for set-point control and trajectory-tracking control with proportional controller been used with kinematic control scheme. The idea behind this analysis is to showcase the behavior of the mobile robot when FTC is used with the identified faults. Current research directions are towards minimizing the error occurred during set-point control and trajectory-tracking control to obtain the desired performance within further minimum tolerance limit.

REFERENCES

1. Han, K.L.; Choi, O.K.; Kim, J.; Kim, H. & Lee J. S. Design and control of mobile robot with mecanum wheel. *In* Proceeding on the ICROS-SICE, Fukuoka, Japan, 2009, pp. 2932–2937.
2. Pin, F. G. & Killough, S. M. A new family of omnidirectional and holonomicwheeled platforms for mobile robots. *IEEE Trans. Robot. Autom.*, 1994, **10**(4), 480–489. doi: 10.1109/70.313098
3. Gfrerrer, A. Geometry and kinematics of the Maronia-Makri active fault.pdf. *Elsevier*, 1975 pp. 1–14.
4. Diegel, O.; Badve, A.; Bright, G.; Potgieter, J. & Tlale, S. Improved mecanum wheel design for omni-directional robots. *In* Proceeding 2002 Australasian Conference on Robotics and automation, Auckland, 2002. pp. 27–29 .
5. Indiveri, G. Swedish wheeled omnidirectional mobile robots: Kinematics analysis and control. *IEEE Trans. Robot.*, 2009, **25**(1), 164–171. doi: 10.1109/TRO.2008.2010360
6. Muir, P. F. & Neuman, C. P. Kinematic modeling of wheeled mobile robots. *J. Field Robotics.* 1987, **4**(2), 281-340. doi: 10.1002/rob.4620040209
7. Gracia, L.; & Tornero, J. Kinematic control of wheeled mobile robots. *Lat. Am. Appl. Res.*, 2008, **38**(1), 7–16.
8. Mohammed, T.B. *et al.* Development of mobile robot drive system using mecanum wheels. 2016 Int. Conf. Adv. Electr. Electron. Syst. Eng. ICAEES 2016, Putrajaya, Malaysia pp. 582–585. doi: 10.1109/ICAEES.2016.7888113
9. Dickerson, S.L. & Lapin, B.D. Control of an omni-directional robotic vehicle with Mecanum wheels. *NTC 91 Natl. Telesystems Conf. Proc.*, 1991, pp. 323–328. doi: 10.1109/NTC.1991.148039
10. Campion, G.; Bastin, G. & D'Andrea-Novel, B. Structural properties and classification of kinematic and dynamic\ nmodels of wheeled mobile robots. *In* Proceeding IEEE Int. Conf. Robot. Autom., 1993, **1**, pp. 462–469. doi: 10.1109/ROBOT.1993.292023
11. Olsen, M.M. & Petersen, H. G. A new method for estimating parameters of a dynamic robot model. *IEEE Trans. Robot. Autom.*, 2001, **17**(1), 95–100. doi: 10.1109/70.917088
12. Zhang, Y. & Jiang, J. Bibliographical review on reconfiguratble fault-tolerant control systems. *IFAC Proc. Vol.*, 2003, **36**(5), 257–268.
13. Zhou D. H. ;& Frank, P. M. Fault diagnostics and fault tolerant control. *Aerosp. Electron. Syst. IEEE Trans.*, 1998, **34**(2), 420–427. doi: 10.1109/7.670324
14. Blanke, M.; Staroswiecki, M. ;& Wu, N.E. Concepts and

methods in fault-tolerant control. *In* Proceeding 2001 Am. Control Conf. (Cat. No.01CH37148), 2001, **4**, pp. 2606–2620.
doi: 10.1109/ACC.2001.946264

15. Vlantis, P.; Bechlioulis, C. P.; Karras, G.; Fourlas, G. & Kyriakopoulos, K. J. Fault tolerant control for omni-directional mobile platforms with 4 mecanum wheels.*In* Proc. - IEEE Int. Conf. Robot. Autom., 2016, pp. 2395–2400.
doi: 10.1109/ICRA.2016.7487389
16. Jiang J. & Yu, X. Fault-tolerant control systems: A comparative study between active and passive approaches. *Ann. Rev. Control*. 2012.
doi: 10.3390/s130811007
17. Yin, S.; Luo, H. & Ding, S. X. Real-time implementation of fault-tolerant control systems with performance optimization *IEEE Trans. Ind. Electron.*, 2014, **61**(5), 2402–2411.
doi: 10.1109/TIE.2013.2273477
18. Blyth, W. A.; Barr, D. R. W. & Baena, F. R. Y. A reduced actuation mecanum wheel platform for pipe inspection. *In* IEEE/ASME Int. Conf. Adv. Intell. Mechatronics, AIM, 2016, pp. 419–424.
doi: 10.1109/AIM.2016.7576803
19. Song, B.; Zhang, Y.; Cheng, J. & Wang, J. Path Following Control of a Mobile Robot via Line-of-Sight Method. *In* 2010 Second Int. Conf. Intell. Human-Machine Syst. Cybern., 2010, pp. 143–146.
doi: 10.1109/IHMSC.2010.135
20. Warwick, K.; Xydas, D.; Nasuto, S.J.; Becerra,V.M.; Hammond,M.W.; Downes, J.H.; Benjamin, S.M. & Whalley, J. Controlling a mobile robot with a biological brain. *Def. Sci. J.*, 2010, **60**(1), pp. 5-14.
21. Jung, E.J.; Yi,B.J. & Kim,W.K. Motion planning algorithms of an omni-directional mobile robot with active caster wheels. *Intell. Serv. Robotics*, 2011, **4**, pp. 167–180.
22. Topiwala, A. Modeling and simulation of a differential drive mobile robot. *Int. J. Sci. Eng. Res.*, 2016, **7**(7), 1410–1415,
23. Contreras, J.C.M.; Herrera, D.; Toibero, J.M. & Carelli, R. Controllers design for differential drive mobile robots based on extended kinematic modeling. 2017 *European Conference on Mobile Robots (ECMR)* Paris, France, 2017, pp. 1-6.
doi: 10.1109/ECMR.2017.8098661
24. Lee, T. C.; Song, K. T.; Lee, C. H. & Teng, C. C. Tracking control of unicycle-modeled mobile robots using a saturation feedback controller. *IEEE Trans. Control Syst. Technol.*, 2001, **9** (2), 305–318.
doi: 10.1109/87.911382
25. Suárez A. & González, L. A generalization of the Moore-Penrose inverse related to matrix subspaces of Cn × m. *Appl. Math. Comput.*, 2010, **216**(2), 514–522.
doi: 10.1016/j.amc.2010.01.062
26. Park, J.; Choi, Y.; Chung, W. K. ; & Youm, Y. Multiple Tasks Kinematics Using Weighted Pseudo-Inverse for Kinematically Redundant Manipulators. *Int. Conf. Robot. Autom.*, 2001,19104. pp. 1033–1036.
doi: 10.1109/ROBOT.2001.933249
27. Tzafestas, S. G. Introduction to Mobile Robot Control. *Elsevier*, October, 2015.

ADDITIONAL INFORMATION

Supplementary information accompanies this paper at https://doi.org/10.14429/dsj.69.13607

ACKNOWLEDGEMENT

This work was supported in part by the Department of Higher Education (Project No.:1-36/2016-PN-II), India.

CONTRIBUTORS

Ms Swati Mishra graduated in Automobile Engineering from Oriental Institute of Science & Technology, Bhopal, Madhya Pradesh, India, in 2010. She did her Master degree in Specialisation of Design and Thermal from Institute of Engineering, D.A.V.V Indore, in 2012. She is currently pursuing PhD in the Discipline of Metallurgy Engineering & Material Science at IIT Indore, India.
In the current study she carried out original draft preparation, collecting the data and editing of the paper.

Mr Mukesh Sharma is a BTech undergraduate student in Department of Mechanical Engineering, IIT Jodhpur, Rajasthan, India (expected 2020). His research interest includes motion planning, vision and machine learning.
In the current study, he carried simulation, programming and supporting algorithms and also helped in writing the draft.

Dr Santhakumar Mohan graduated from GCE Salem in 2003. He received his Master's from GCT Coimbatore in 2005. He got his PhD (Robotics and Control) from IIT Madras in 2010. He worked as an Associate professor at IIT Indore. Currently, he is working as an Associate professor at IIT Palakkad. He is holding visiting faculty positions at IISc Bangalore, India, RWTH Aachen, Germany and ECN, France. His active research areas include underwater vehicle and underwater manipulator design and control, parallel robotic platforms, assistive robots, field and service robots, intelligent motion control, and, dynamic modelling and control of dynamic systems.
In the current study, he guided in the formulation of concept and research objectives, analysis of data and execution of experiment and draft.